Dynamic Effects of Shock-Induced Flow Separation

Lars E. Ericsson*
Lockheed Missiles and Space Company, Inc., Sunnyvale, Calif.

Shock-induced flow separation is the flow mechanism usually responsible for what the structural dynamicist terms "buffet." The shock-induced flow separation affects the aeroelastic response via two different mechanisms: 1) The flow separation generates fluctuating pressures, i.e., a forcing function that is independent of the motion of the aerodynamic surface; e.g., an aircraft wing, and 2) the flow separation affects the motion-dependent forces and can in some cases generate negative aerodynamic damping. A simple analysis is presented which, using static experimental data as an input, can predict these two buffet-components for a wing in high Mach number subsonic flow.

Nomenclature

a = speed of sound
b = wing span
c and $\bar{c}$ = reference length, c = 2-dim. chord length $\bar{c} = S/b$, mean aerodynamic chord
k_a = dynamic overshoot coefficient, Eq. (26)
K, k = reduced frequencies of shock boundary layer interactions, Eqs. (19) and (20), respectively.
L, l = separation lengths, see Fig. 7
l = section lift, coefficient $c_l = l/(\rho_\infty U^2_\infty/2)c$
M = Mach number, $M = U/a$
M_p = pitching moment, coefficient $C_m = M_p/(\rho_\infty U^2_\infty/2)Sc$
m_p = section pitching moment, coefficient $c_m = m_p/(\rho_\infty U^2_\infty/2)c^2$
N = normal force, coefficient $C_N = N/(\rho_\infty U^2_\infty/2)S$
n = section normal force, coefficient $c_n/(\rho_\infty U^2_\infty/2)c$
η = exponent for viscosity-temperature relationship, $\eta = 3/4$
p = static pressure, coefficient $C_p = (p - p_\infty)/(\rho_\infty U^2_\infty/2)$
S = reference area
S_e = density ratio, $S_e = \rho_e/\rho_{wall}$, Eq. (21)
t = time
T = period of oscillation
U = velocity
$\bar{U}$ = convection velocity
U_w = apparent wall velocity
x = horizontal coordinate
z = translatory coordinate
α = angle of attack
$\tilde{\alpha}$ = generalized angle of attack, Eq. (25)
$\Delta\alpha_s$ = stall delay due to "leading edge jet" effect, Eq. (26)
γ = ratio of specific heats, $\gamma = 1.4$ in air
Δ = increment
ζ = damping, fraction of critical
θ = pitch perturbation
ξ = dimensionless x-coordinate, $\xi = x/c$
ξ_{CG} = center of pitch oscillation
ρ = air density
σ = bending mode response amplitude
τ = dimensionless time, $\tau = U_\infty t/c$
ω = angular oscillation frequency
$\bar{\omega}$ = reduced frequency, $\bar{\omega} = \omega c/U_\infty$ (or $\omega\bar{c}/U_\infty$)

Subscripts

a = accelerated flow effect
$c.g.$ = center of gravity
e = boundary-layer edge conditions
j = jet effect
L = local
s = flow separation
sh = shock
t = total
∞ = undistrubed flow

Superscripts

i = induced e.g., $\Delta^i c_n$ = separation-induced sectional normal force
$\hat{}$ = value aft of a normal shock, e.g., $\hat{p}_e$

Differential Symbols

$\dot{\alpha} = \partial\alpha/\partial t; \xi' = \partial\xi/\partial\tau$

$c_{n\alpha} = \partial c_n/\partial\alpha$

$c_{n\dot{z}} = dc_n/d(\dot{z}/U_\infty)$

Presented as Paper 73-308 at the AIAA Dynamics Specialists Conference, Williamsburg, Va., March 19-20, 1973; submitted July 9, 1973; revision received April 5, 1974. The flow concepts used in the paper were in part developed in studies for NASA under Contracts NAS 8-11238, NAS 8-20354, NAS 9-11445, NAS 1-6450, NAS I-7999, and NAS 1-9987.

Index categories: Nonsteady Aerodynamics; Subsonic and Transonic Flow; Aircraft Vibration.

*Consulting Engineer. Associate Fellow AIAA.

Introduction

DURING a recent AGARD meeting, J.G. Jones[1] brought up the age-old problem of how to define "buffet." The usual definition is that the separation-induced forcing function is the dominant effect, and that changes in the aerodynamic damping are of negligible magnitude. However, both effects are often of equal significance. Jones[1] showed that at buffet onset on a moderately swept wing a large increase of the (apparent) aerodynamic damping was observed (Fig. 1). However, the straight wing on an early space shuttle configuration experiences negative aerodynamic damping at a slightly higher subsonic Mach number[2] (Fig. 2). Those two recent examples serve to illustrate the complexity of the dynamic effects caused by shock-induced flow separation. An analysis is presented that hopefully will provide a better understanding of this complex flow phonomenon.

Analytic Approach

The shock-induced flow separation affects the vehicle response via two different mechanisms. 1) The flow separation generates fluctuating pressures, i.e., a forcing function that is independent of the vehicle response. 2) The

flow separation affects the motion dependent forces and can sometimes generate negative aerodynamic damping.

The experimental data obtained by Lambourne[3] for the effect of pitch-up rate on leeward side shock position on a moderately thick airfoil at $M=0.7$, presented by W. P. Jones in his Minta Martin Lecture,[4] illustrates the two facets of the buffet problem (Fig. 3). The data show that when the angle of attack is increased at a constant rate, $c\dot{\alpha}/U_\infty = 0.0059$, the shock is lagging the airfoil motion. The shock is also exhibiting high frequency oscillations around the mean, motion-dependent position. If one could predict analytically the measured shock position, both the mean, motion-dependent location and the superimposed oscillation, one would obviously have taken a big step towards the development of analytic methods for prediction of wing buffet. Such an analysis will now be described.

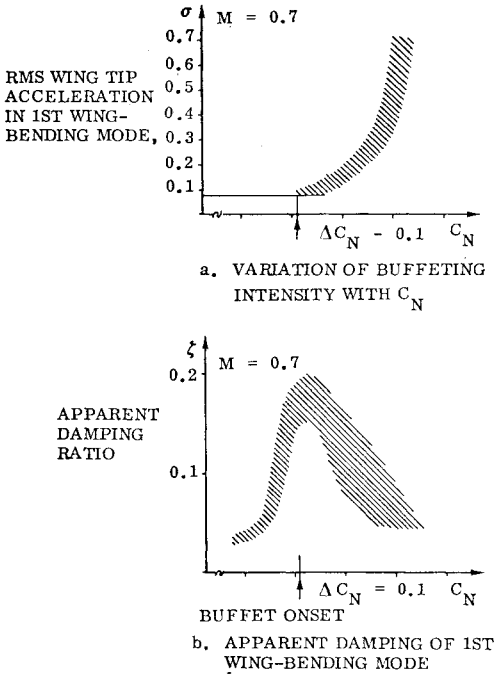

Fig. 1 Flight test data of wing buffet.[1]

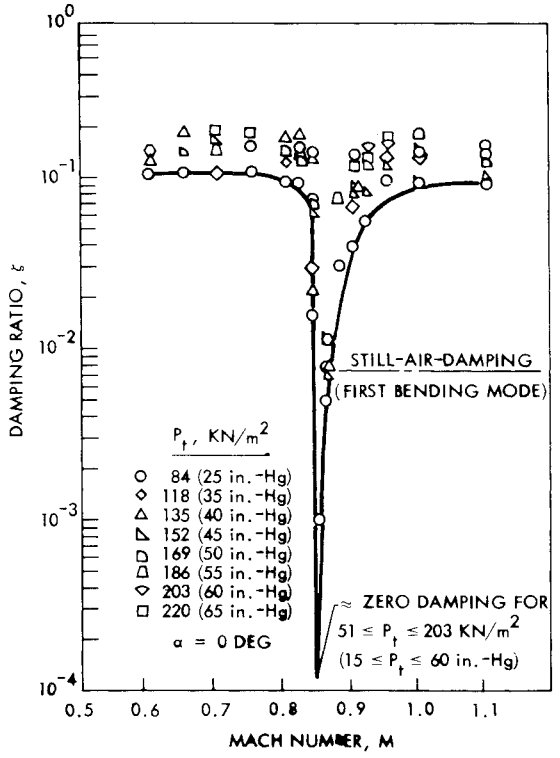

Fig. 2 Effect of Mach number on the damping in bending of a straight wing.[2]

Analysis

Three factors determine when and where flow separation occurs. They are 1) boundary-layer profile shape, 2) boundary-layer thickness, and 3) adversity of local pressure gradient. In the case of shock-induced separation on cone-cylinder bodies[5,6] the first two factors are determined by forebody crossflow effects, which in the dynamic case lag the instantaneous (corresponding static) values owing to the convective time lag in the boundary layer buildup. The adversity of the local pressure gradient also lags the instantaneous value due to accelerated flow effects.

In the case of an airfoil in pitch-up motion, there are no cross flow effects, and both profile shape and boundary-layer thickness are determined by the pressure gradient time history upstream of separation[7] and by motion-induced moving wall effects.[7] Thus, the dependence of the pressure gradient on the airfoil motion is of primary concern. The adversity of the pressure gradient is determined by the circulation, and the lag in the dynamic case is caused by the Karman-Sears wake lag.[8,9] In the case of shock-induced separation there is an additional delay of the adversity caused by the shock movement. The shock is moving forward relative to the airfoil surface with a speed that can be expressed as follows:

$$\Delta U_{sh} = c\dot{\xi}_{sh} = -(\partial \xi_{sh}/\partial \alpha)c\dot{\alpha} \tag{1}$$

That is, the Mach number ahead of the shock is increased by the amount

$$\Delta M_{sh}/M_e = \Delta U_{sh}/U_e = -(\partial \xi_{sh}/\partial \alpha)(c\dot{\alpha}/U_e) \tag{2}$$

Figure 3b shows that the increase in Mach number will slow the forward shock movement down by the amount

$$\Delta \xi_{sh}(M_{sh}) = (\partial \xi_{sh}/\partial M_\infty)(M_\infty/M_e)\Delta M_{sh} \tag{3}$$

The angle of attack can, therefore, be exceeded by the amount

$$\Delta \alpha(M_{sh}) = \dot{\alpha}\Delta t_{sh} = \xi_{ash}(c\dot{\alpha}/U_e) \tag{4}$$

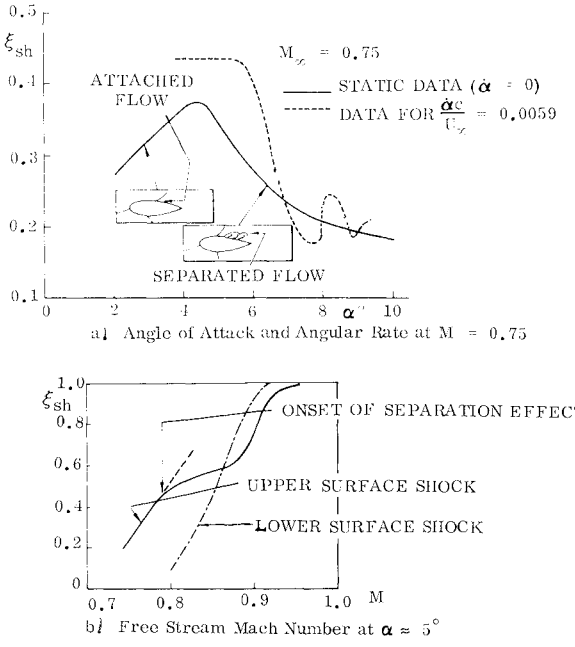

Fig. 3 Effects of flow parameters on shock boundary-layer interaction.[3]

Equations (2)-(4) define the following value for the shock motion induced equivalent time lag† ξ_{ash}

$$\xi_{ash} = (\partial \xi_{sh}/\partial M_\infty) M_\infty \tag{5}$$

The quasi-steady (mean) lag $\Delta\xi_{sh}$ of the shock induced separation, corresponding to $\Delta\alpha(M_{sh})$, is simply

$$\Delta\xi_{sh}(M_{sh}) = (\partial \xi_{sh}/\partial\alpha)\Delta\alpha(M_{sh}) \tag{6}$$

There is yet another mechanism for coupling between the separation movement and the external flowfield. Moore[10] has discussed such a flow mechanism. When the separation point moves upstream, the boundary layer, ready to separate, sees a downstream moving wall, and the beneficial effects on the boundary layer delays the flow separation. The apparent wall velocity is given by Eq. (1), i.e., $U_w = \Delta U_{sh}$. The separation will lag its static position due to this moving wall effect by

$$\Delta\xi_s\left(\frac{U_w}{U_\infty}\right) = \partial\xi_s/\left[\partial\left(\frac{U_w}{U_\infty}\right)\right]\frac{U_w}{U_\infty} \tag{7}$$

The corresponding overshoot $\Delta\alpha(U_w/U_\infty)$ is given by an equation like Eq. (4), where

$$\xi_{as} = \partial\xi_s/\partial\left(\frac{U_w}{U_\infty}\right) \tag{8}$$

Using rotating cylinder data obtained by Brady and Ludwig[11] one obtains for the airfoil‡ (Fig. 4)

$$\partial\xi_s/\partial\left(\frac{U_w}{U}\right) \approx \begin{cases} 0.7; \text{ supercritical Reynolds numbers} \\ 3.0; \text{ subcritical Reynolds numbers} \end{cases} \tag{9}$$

The supercritical case is representative of (shock-induced) separation near the trailing edge. This lag, ξ_{as}, due to separation movement, should be added to the lags ξ_{ash} and ξ_w, due to shock movement and vortex wake lag, respectively. Thus, the total lag angle $\Delta\alpha$ is§

$$\Delta\alpha(\Delta t) = -\dot{\alpha}\Delta t = -(\xi_{ash} + \xi_{as} + \xi_w)(c\dot{\alpha}/U_\infty) \tag{10}$$

†Note that $\Delta\xi_{sh} = (\partial\xi_{sh}/\partial\alpha)\Delta\alpha$.

‡Airfoil-like pressure distribution was impressed upon the rotating cylinder by the use of a shroud.[11]

§The convective time lag Δt_c, Eq. (9) in Ref. 24, has been neglected. It would increase Δt by approximately 10%.

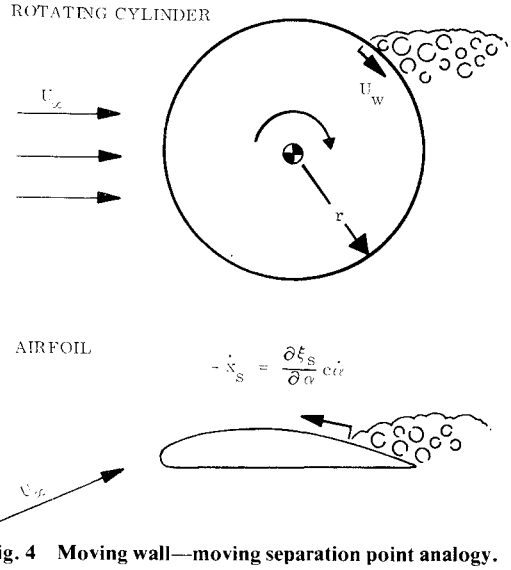

Fig. 4 Moving wall—moving separation point analogy.

It was shown in Ref. 9 that the Karman-Sears vortex wake lag is $\xi_w = 1.5$. Figure 3b gives $\partial\xi_{sh}/\partial M_\infty = 1.2$ for $M_\infty = 0.75$, which in Eq. (5) gives $\xi_{ash} = 0.9$.

Figure 3a gives

$$\partial\xi_s/\partial\alpha = \begin{cases} -4.0 \text{ at } \alpha = 5^\circ \\ -0.8 \text{ at } \alpha = 10^\circ \end{cases}$$

For $c\dot{\alpha}/U_\infty = 0.0059$ the above data give, with use of equations such as Eq. (6) and Eq. (10), the following values for the mean lag of the shock position in Fig. 3a.

$$\Delta\xi_s = \begin{cases} 0.073 \text{ at } \alpha = 5^\circ \\ 0.013 \text{ at } \alpha = 10^\circ \end{cases}$$

The quasi-steady position is indicated by the dash-dot line in Fig. 5. It seems to indicate a realistic mean position for the measured shock oscillation. The deviation is a high frequency oscillation for which the amplitude decreases and the frequency increases when the angle of attack is increased. The α-half periods for the four cycles shown are

$$\Delta\alpha = 2.5^\circ,\ 1.3^\circ,\ 0.7^\circ, \text{ and } 0.5^\circ$$

The corresponding reduced frequencies are

$$\bar{\omega} = \frac{\omega c}{U_\infty} = \frac{\pi}{\Delta\alpha}\frac{\dot{\alpha}c}{U_\infty} = \frac{180}{\Delta\alpha^\circ}\frac{\dot{\alpha}c}{U_\infty}$$

$$= 0.425,\ 0.815,\ 1.52, \text{ and } 2.13$$

Examining this high frequency oscillation further reveals that its amplitude and frequency vary with angle of attack in a manner prescribed by the separation sensitivity to angular changes, i.e., $\partial\xi_s/\partial\alpha$. This is demonstrated in Fig. 6, which shows that

$$|\xi_s|_{osc} \approx 0.025\partial\xi_s/\partial\alpha \tag{11}$$

$$|\xi_s|_{osc}\bar{\omega}_{osc} \approx 0.043 \tag{12}$$

As Trilling[12] has shown that shock-boundary layer interactions can generate harmonic self-sustained oscillations, one may suspect that these shock oscillations are of pseudoharmonic nature.¶ Such an oscillation can be expressed as

$$\frac{d^2\Delta^i\xi_s}{dt^2} + 2\zeta\omega\frac{d\Delta^i\xi_s}{dt} + \omega^2\Delta^i\xi_s = 0 \tag{13}$$

where

$$\Delta^i\xi_s = \xi_s - (\xi_s)_{mean}$$

¶With slowly changing "environment" $(\partial\xi_{sh}/\partial\alpha) = f(\alpha)$, which can be considered constant for one half cycle of oscillation.

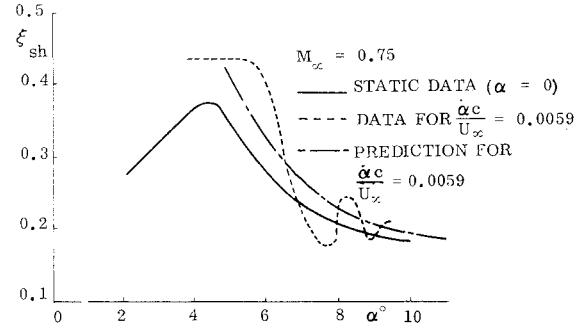

Fig. 5 Comparison between predicted and measured unsteady shock position.

Using the dimensionless time $\tau=(U_\infty/c)t$ (time unit = time for airfoil to travel one chord length), Eq. (13) becomes

$$\frac{d^2\Delta^i\xi_s}{d\tau^2}+2\zeta\bar{\omega}\frac{d\Delta^i\xi_s}{d\tau}+\bar{\omega}^2\Delta^i\xi_s=0 \tag{14}$$

The solution to Eq. (14) is (see, for example, Ref. 13)

$$\Delta^i\xi_s(\tau)=[\Delta^i\overset{\circ}{\xi}_s(0)/\bar{\omega}^2(1-\zeta^2)^{1/2}]$$

$$\exp(-\zeta\bar{\omega}\tau)\sin(\bar{\omega}\tau[1-\zeta^2]^{1/2}) \tag{15}$$

where $\Delta^i\overset{\circ}{\xi}_s(0)=0$ and $d\Delta^i\xi_s(0)/d\tau=\Delta^i\dot{\xi}_s(0)$ are the initial conditions. With the classical assumption that the damping as a fraction of critical, ζ, is small, $\zeta^2\ll1$, Eq. (15) becomes

$$\Delta^i\xi_s(\tau)=[\Delta^i\overset{\circ}{\xi}_s(0)/\bar{\omega}]\exp(-\zeta\bar{\omega}\tau)\sin(\bar{\omega}\tau) \tag{16}$$

With $\bar{\omega}\zeta=0(\zeta)$ the effect of the exponential decay can be neglected and the oscillation amplitude obeys the relationship

$$|\Delta^i\xi_s|\,\bar{\omega}=\Delta^i\overset{\circ}{\xi}_s(0)=\text{constant} \tag{17}$$

The initial rate $\Delta^i\overset{\circ}{\xi}_s(0)$ is

$$\Delta^i\overset{\circ}{\xi}_s(0)=(\partial\Delta^i\xi_s/\partial\alpha)(c\dot{\alpha}/U_\infty)$$

$$\partial\Delta^i\xi_s/\partial\alpha=\partial\xi_{sh}/\partial\alpha-\partial\xi_s/\partial\alpha \tag{18}$$

From Fig. 3a are obtained the shock derivatives at $\alpha=5°$, the initial conditions at time of initiation of the shock oscillation.

$$\partial\xi_{sh}/\partial\alpha=2.9;\ \partial\xi_s/\partial\alpha=-4.2$$

For $c\dot{\alpha}/U_\infty=0.0059$, Eq. (18) gives $\Delta^i\overset{\circ}{\xi}_s(0)=0.042$, and Eq. (17) becomes

$$|\Delta^i\xi_s|\bar{\omega}=0.042$$

which is in excellent agreement with the experimentally observed value, Eq. (12).

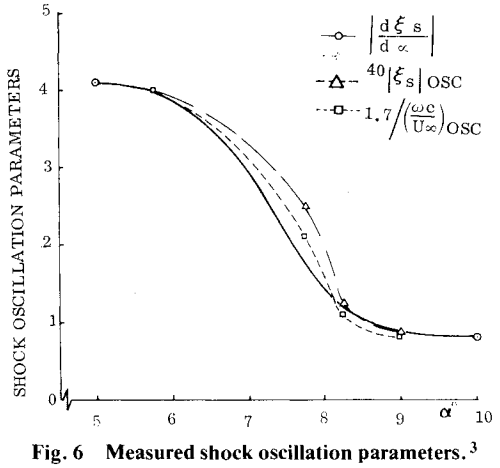

Fig. 6 Measured shock oscillation parameters.[3]

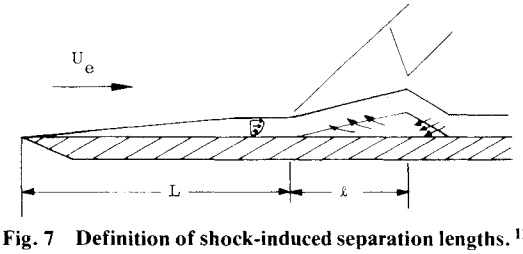

Fig. 7 Definition of shock-induced separation lengths.[12]

The self-sustained oscillations for laminar shock-boundary interactions, predicted by Trilling[12] and measured by Fizdon,[14] have characteristic frequencies that can be defined in two alternate ways (Ref. 12 and Fig. 7)

$$K=\omega l/U_\infty \tag{19}$$

$$k=\omega L/U_\infty=K/2S^{\eta}_e(\Delta C_{psh})_e \tag{20}$$

where $K=1.79$ is the value for the lowest harmonic. Only when the shock has moved away from the trailing edge (control) can one expect the shock oscillation to be similar to the free interaction case treated by Trilling. At $\alpha=10°$ the trailing edge influence, as reflected in $\partial\xi_s/\partial\alpha$, has dropped drastically and the similarity may exist. Substituting $\xi_s c$ for L one gets

$$K=\bar{\omega}\xi_s=K/2S^{\eta}_e(\Delta C_{psh})_e \tag{21a}$$

$$S_e=\rho_e/\rho_{wall}=(1+0.2M_e^2)^{-2.5} \tag{21b}$$

$$(\Delta C_{psh})_e=[(\hat{p}_e/p_e)-1]/0.7M_e^2 \tag{21c}$$

$\hat{p}_e/p_e\approx1.4$ for incipient shock induced separation,[15] and $1.35<\hat{p}_e/p_e<1.6$ for shock-augmented leading edge stall (Fig. 8).[16] Assuming a normal shock for determination of M_e associated with $\hat{p}_e/p_e$, Eqs. (21) give with $n\approx3/4$[17] and $K=1.79$[12] the following value for k: $0.41<k<0.62$. With $\xi_s\approx0.2$ the value for $\bar{\omega}$ is $2.05<\bar{\omega}<3.1$.

The measured value was $\bar{\omega}=2.13$. Looking at Fig. 8, one would assume that the most forward shock location, for which the boundary layer at separation is laminar (shock augmented L.E. stall), should compare best with Trilling's laminar analysis. Assuming that the stall at $\alpha=10°$ in Fig. 5 also is a shock-augmented leading edge stall, one would pick the low value $\bar{\omega}=2.05$, which would give a good prediction of the measured frequency $\bar{\omega}=2.13$.**

When the shock is closer to the trailing edge, e.g., at $\alpha=5°$ in Fig. 5, it is a wake-dominated situation[15] somewhat similar to that for aft body separation off bulbous bases.[19] For the starting "large bubble"[15] separation at $\alpha=5°$ one can assume the "wake neck" to be near the trailing edge, and l in Eq. (19) can be approximated by the distance from separation to trailing edge and back again.

$$k=2\bar{\omega}(1-\xi_s)/(\bar{U}/U_\infty) \tag{22}$$

The other limit for advanced "large bubble" separation could be approximated by twice this distance. With $K=1.79$, $\bar{\omega}=0.425$, and $\xi_s=0.35$, Eq. (22) gives

$$0.31<\bar{U}/U_\infty<0.62$$

which looks reasonable.[20]

**This frequency is too high to drive the wing bending, but is of the right magnitude to drive the wing torsional degree of freedom. However, at $\alpha=5°$ the frequency is $\bar{\omega}=0.425$, which could drive the wing bending. It is assumed, of course, that the wing remains at a nearly constant angle of attack, i.e., the shock oscillations are harmonic and not nonlinear in character as in Lambourne's experiment.

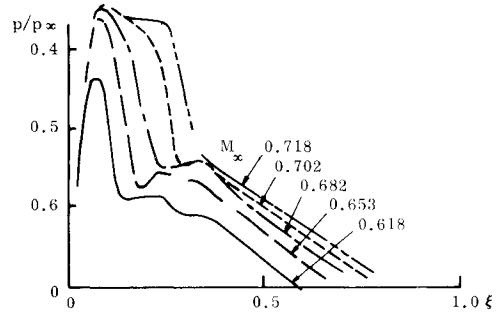

Fig. 8 Effect of Mach number on shock-induced separation at $\alpha=3°$.[16]

It is interesting to compare Ham's pitch-up airfoil data[21] at $M \ll 1$ (Fig. 9) with those of Lambourne[3] at $M=0.7$ (Fig. 5). They show very similar characteristics. It appears that the moving-separation-point effect (Fig. 4) supplies the coupling corresponding to the moving-shock effect used in Trilling's analysis.[12] The "spilled" leading edge vortex[22] will generate transient lift during its travel over the chord, as will an elongating separation bubble,[23] but neither flow mechanism would generate any oscillatory behavior. The reduced frequencies of the three half cycles are $\bar{\omega}=2.0$, 2.75, and 5.0, i.e., somewhat higher than for the shock-induced separation investigated by Lambourne.

To compute the unsteady aerodynamics, one needs to determine the force change associated with the shock induced separation movement. According to Pearcey,[15] the strength of the shock remains relatively constant, as it is determined by the pressure increase that the upstream boundary layer can stand without separation. This would be true at the "turning point," $\xi_{sh}=0.35$ in Fig. 3a, where the pressure gradient upstream of the shock is relatively mild. That is, the boundary-layer shape and thickness remain relatively unchanged. This pressure ratio for incipient separation[15] is $\hat{p}_e/p_e=1.4$.

Before the "turning point," $\alpha=5°$ in Fig. 5, the shock induced attached flow loading is

$$\Delta^i c_{n\alpha sh}=\Delta C_{psh}\,(d\Delta^i\xi_s/d\alpha)$$

$$\Delta C_{psh}=[\,(\hat{p}_e/p_e)-1\,]\,(2/\gamma M_\infty^2)\,(p_e/p_\infty) \qquad (23)$$

$$=(4.7)(1/M_\infty^2)[\,(1+0.2M_\infty^2)/(1+0.2M_e^2)\,]^{3.5}$$

$M_e \approx 1.16$ for $\hat{p}_e/p_e=1.4$ through a normal shock.

After the "turning point," the separation-induced load $\Delta^i c_{n\alpha s}$ that detracts from the attached flow lift, $c_{n\alpha L}+\Delta^i c_{n\alpha sh}$, is as follows

$$\Delta^i c_{n\alpha s}=\Delta C_{psh}\,[\,(d\xi_{sh}/d\alpha)-$$

$$(d\xi_s/d\alpha)\,]=C_{psh}\,(d\Delta^i\xi_s/d\alpha) \qquad (24)$$

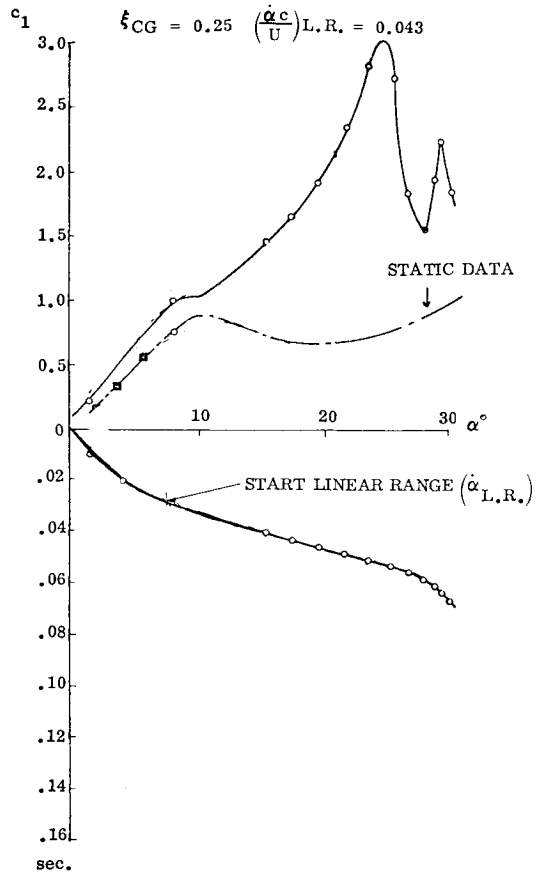

Fig. 9 Effect of ramp-wise change of angle of attack on NACA-0012 airfoil stall.[21]

How the unsteady loads for the pitching degree of freedom are obtained has been shown before.[7,9,22] In the present case one is interested also in the wing bending degree of freedom, i.e., the plunging degree of freedom for the airfoil section, and the generalized angle of attack for a straight wing is

$$\tilde{\alpha}=\alpha+\theta+(\xi-\xi_{c.g})\,(c\dot{\theta}/U_\infty)+\dot{z}/U_\infty \qquad (25)$$

It was found in the analysis reported earlier[7,24] that a leading edge wall-jet effect was the only mechanism that explains the dynamic improvement of the boundary layer for the plunging airfoil (see Fig. 10). In this case $\Delta\alpha_s$ can be expressed as follows:

$$\Delta\alpha_s=k_a\,(U_{wj}/U_\infty)$$

$$(U_{wj}/U_\infty)=(\dot{z}/U_\infty)\} \qquad (26)$$

With $k_a=4$ for this leading edge jet effect the aerodynamic undamping in plunge measured by Liiva et al.[21] can be predicted.[26] Although the data in Ref. 25 show that the dynamic stall overshoot of $c_{l\max}$ disappears at $M=0.6$, which is in agreement with the results obtained on airplane models in pitch-up motion,[7,27] it could still cause an "extra overshoot" of the static α_s before the shock induced separation in the dynamic case reaches the same location ξ_s. This is implied by the observed effects of boundary layer profile and thickness changes due to transition near the leading edge.[28,29]

For pure bending oscillations the sectional plunging force coefficient is simply $c_{n\dot{z}}\,(\dot{z}/U_\infty)$, where

$$c_{n\dot{z}}=\frac{\partial c_n}{\partial(\dot{z}/U_\infty)}=c_{n\alpha}=c_{n\alpha L}+\Delta^i c_{n\alpha sh}+\Delta^i c_{n\alpha s} \qquad (27)$$

For $M_\infty=0.75$, $\Delta C_{psh}=0.89$. Using the slopes from Fig. 3a, Eqs. (23) and (24) give

$$\Delta^i c_{n\alpha sh}=2.6;\ \Delta^i c_{n\alpha s}=-6.35$$

With

$$c_{n\alpha}=c_{n\alpha_0}\,(1-M_\infty^2)^{1/2}=5.7/(1-M_\infty^2)^{1/2}$$

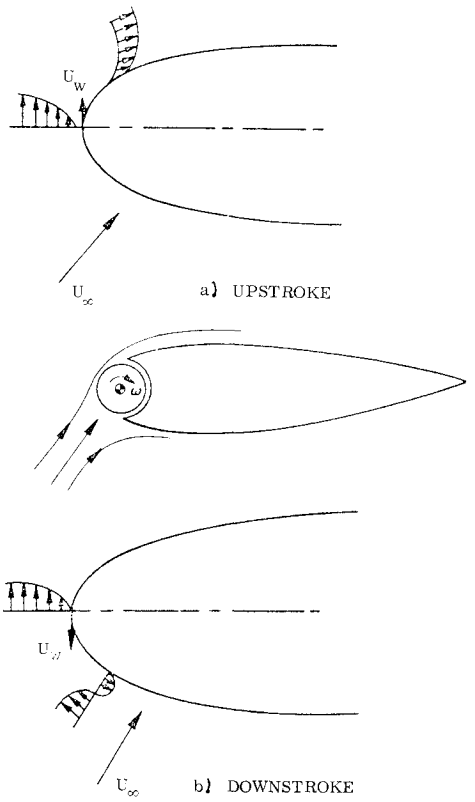

Fig. 10 Pitch rate induced decelerating wall effect.

That is, when approaching the "turning point," $\alpha<5°$ in Fig. 5, the "apparent damping" would increase by 37%, and decrease past the "turning point," $\alpha>5°$ in Fig. 3a, to 53% below the original damping level for lower angles of attack. This trend is in qualitative agreement with the data in Fig. 1, but the magnitudes are all wrong. The apparent damping in Fig. 1 increases much more than 37%. The data in Fig. 3a, which were used to give the shock movement derivatives, are for a relatively thick airfoil. The data in Fig. 1 are for a much thinner (7% thick) airfoil designed for transonic flight. This probably means that the pressure distribution over the foreward portion is very flat, and not steeply adverse as is the case for a standard thick airfoil designed for low speed. As a result the shock movement derivatives would be much larger than those obtained form the thick airfoil data in Fig. 3a.

Also, the data in Fig. 1 are for a swept wing, and three-dimensional flow effects could account for some of the above differences in magnitude. Hall and Rogers[30] have shown a mechanism that can amplify the section characteristics: the spanwise extent of the outer, single, strong shock changes with angle of attack, thus adding a new dimension to the strip-effects discussed earlier. There are also other three dimensional flow phenomena[31] that possibly could explain the tremendous damping increase observed by Jones (Fig. 1) (see Ref. 32 for a detailed discussion).

Another way of amplifying the pure plunging effects discussed above is pointed out by Erickson et al.[2,33] When the elastic axis does not coincide with the center of gravity, the bending will induce a wing twist. When the elastic axis is forward of the center of gravity, as was the case in their tests[2,33] the leading edge is twisted up during the down stroke of the oscillation. That is, the plunge-induced angle of attack $\dot{z}/U_\infty$ is augmented by the sectional pitch angle due to twist. Note that this twisting oscillation is driven by the bending oscillation and, as a consequence, is completely in phase with the bending oscillation regardless of the (usual) large difference in natural frequencies between the bending and torsional wing modes. A similar augmenting of the plunging effect is obtained through sweep back.

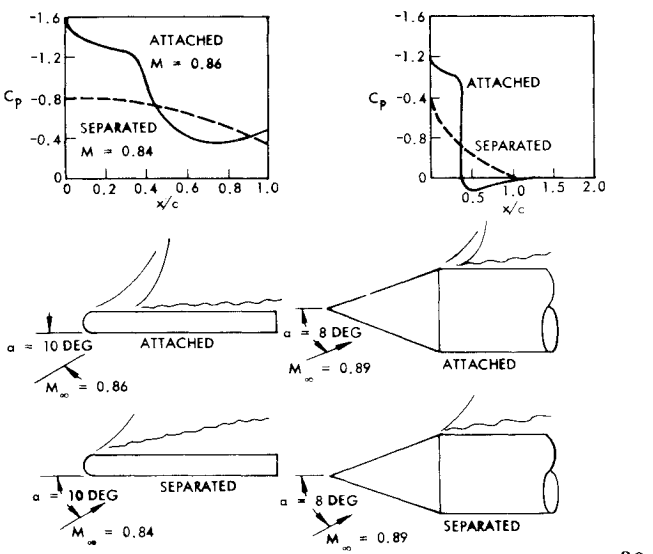

a) SLAB WING[34] b) 15-DEG CONE-CYLINDER[36]

Fig. 11 Comparison of pressure distributions for sudden separation in two- and three-dimensional flow.

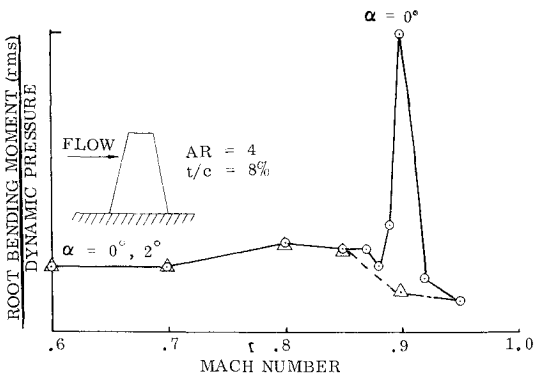

Fig. 12 Dynamic instability of vertical fins.[33-37]

If the angle of attack was increased above $\alpha=10°$ in Fig. 3a at a certain critical α the shock would jump to the leading edge to cause nose stall. Every airfoil has a critical α-M boundary at high subsonic speed for which this jump occurs.[34] Near this critical boundary self-sustained oscillations could result due to generated negative damping for wing bending with or without associated wing twist. The oscillations observed on the straight wing of a candidate space shuttle geometry both at $M=0.6$, $\alpha=8°$[35] and at $M=0.85$ $\alpha=0$[2] (Fig. 2) could have been caused in this manner. This sudden separation effect is very similar to that on cone-cylinder bodies[36] (Fig. 11). In the latter case, it has been shown[5] that launch vehicle "buffet" results as a consequence of negative aerodynamic damping.†† Again, this is only realized in a very narrow α-M range, very similar to the situation for the wing in Fig. 2. Recently, similar results have been presented for a tapered wing (or actually fin)[33,37] (see Fig. 12).

Although the shock-induced separation did not degrade the aerodynamic damping enough at $\alpha=2°$ to overcome the structural damping and cause any large amplitude bending movement response, the data in Ref. 33 show the decrement to be substantial, more than 60% decrease from the damping level existing at $M\leq0.85$ and $M=0.95$. A possible explanation for the large effect at $\alpha=0$ is that the sudden nose stall may occur (alternatingly) on both sides of the airfoil at $\alpha=0$ causing roughly twice the undamping measured at $\alpha=2°$. These results were obtained using boundary-layer trips near the leading edge. Without trips the transitional boundary layer existing forward of the shock at a certain critical Reynolds number is easier to separate, and, consequently the separation will jump to the leading edge from a more aft position than with trips on. The correspondingly increased separation induced local change could well have caused the violent structural response that destroyed the model.[33] One might suspect that without trips the undamping effect of the shock-induced separation would have been large enough to overcome the structural damping also at $\alpha=2°$. The point is that one can expect negative aerodynamic damping over a narrow α-range as well as over a narrow M-range. That the scaling of these transonic flow phenomena is a big problem, is now a well-known fact.[28,29] The only thing to add is that the problem becomes much more severe when considering the dynamic effects of shock-induced flow separation.[7,38] Figure 18 of Ref. 33 illustrates the fact that the separation induced forcing function and the degradation of aerodynamic damping often are equally important in determining the structural response.

On a real aircraft wing the separated flow patterns may be still more involved,[39,40] and it is of course possible that more complicated flow mechanisms than those described here are responsible for the buffet behavior exhibited in Fig. 1. Moss[40] goes into this question in some detail. Especially interesting is his suggestion that secondary effects caused by the primary motion can be more important than the direct effects, i.e., the single degree-of-freedom response discussed in the present paper. He thinks, for example, that a slight profile change near the leading edge, as a result of wing bending, could have larger effect than the bending itself at the near stall conditions of interest for buffet analysis. The observed large effects of minute leading edge changes on $c_{l_{max}}$[7,41] strongly support the Moss-hypothesis.

††No one has suggested the term launch vehicle flutter for this form of self-sustained oscillations.

Conclusions

The shock induced boundary-layer separation and associated unsteady aerodynamic characteristics causing excessive structural response have been described analytically using static experimental data to define shock movement and separation induced loads.

The shock-induced separation lags the instantaneous (corresponding static) position owing to three unsteady flow effects: 1) the regular Karman-Sears wake lag, 2) the moving wall-moving separation point analogy, and 3) the shock motion induced Mach number change.

The perturbation of the shock-induced boundary-layer separation causes high frequency self-sustained oscillations that can be described analytically, using static experimental shock-position-data as an input. It can be shown that when the shock is near the leading edge, the self-sustained oscillations are of the type described by Trilling for laminar boundary layers. When the shock is farther away from the leading edge, the separation is no longer of the free interaction type but is controlled by the trailing edge and near wake flow conditions.

References

[1] Jones, J. G., "The Dynamic Analysis of Buffeting and Related Phenomena," Paper 23, AGARD-CPP-102, 1972.

[2] Erickson, L. L., Gambucci, B. J., and Wilcox, P. R., "Effects of Space Shuttle Configurations on Wing Buffet and Flutter, Part II, Thick High-Aspect Ratio Wing," *NASA Space Shuttle Technology Conference, Vol. III: Dynamics and Aeroelasticity,* TM X-2274, 1971, pp. 201-229, NASA.

[3] Lambourne, N. C., "Some Instabilities Arising from the Interaction Between Shock Waves and Boundary Layers," C. P. 473, Feb. 1958, Aeronautical Research Council, London.

[4] Jones, W. P., "Research on Unsteady Flow," The Sixth Minta Martin Lecture, *Journal of Aerospace Sciences,* Vol. 29, No. 3, March 1962, pp. 249-263.

[5] Ericsson, L. E., "Aeroelastic Instability Caused by Slender Payloads," *Journal of Spacecraft and Rockets,* Vol. 4, No. 1, Jan. 1967, pp. 65-73.

[6] Ericsson, L. E., "Loads Induced by Terminal-Shock Boundary-Layer Interaction on Cone-Cylinder Bodies," *Journal of Spacecraft and Rockets,* Vol. 7, No. 9, Sept. 1970, pp. 1106-1112.

[7] Ericsson, L. E. and Reding, J. P., "Unsteady Airfoil Stall and Stall Flutter," CR-111906, June 1971, NASA.

[8] von Karman, Th. and Sears, W. R., "Airfoil Theory for Non-Uniform Motion," *Journal Aeronautical Sciences,* Vol. 5, No. 10, Aug. 1938, pp. 379-390.

[9] Ericsson, L. E. and Reding, J. P., "Unsteady Airfoil Stall, Review and Extension," *Journal of Aircraft,* Vol. 8, No. 8, Aug. 1971, pp. 609-616.

[10] Moore, F. K., "On the Separation of the Unsteady Laminar Boundary Layer," *IUTAM Symposium on Boundary Layer Research,* F.R. Germany, 1957, pp. 296-311.

[11] Brady, W. G. and Ludwig, G. R., "Basic Studies of Rotating Stall and an Investigation of Flow-Instability Sensing Devices," AF APL-TR-65-115, Oct. 1965, Air Force Aero Propulsion Lab., Wright-Patterson Air Force Base, Ohio.

[12] Trilling, L., "Oscillating Shock Boundary-Layer Interaction," *Jounral of Aerospace Sciences,* Vol. 25, No. 5, May 1958, pp. 301-304.

[13] Churchill, R. V., "Operational Mathematics," McGraw-Hill, New York, 2nd ed., 1958.

[14] Frizdon, W., "Some Experimental Results of Generating High Frequency Oscillating Shock-Waves and Oscillating Shock-Wave Boundary-Layer Interaction at Supersonic Speeds," *Advances in Aerodynamic Sciences,* Vol. 3, Pergamon Press, New York, 1962, pp. 433-446.

[15] Pearcey, H. H., "Some Effects of Shock-Induced Separation of Turbulent Boundary-Layers in Transonic Flow Past Airfoils," *Paper 9, Proceedings of Symposium on Boundary Layer Effects in Aerodynamics,* National Physics Lab., Great Britain, 1955.

[16] dePaul, V., "Recherches sur des Profils Transsoniques de Faible Trainee," Association Francaise des Ingenieurs et Techniciens de l'Aeronautique et de l'Espace, 4th Colloque d'Aerodynamique Appliquee, 1967, Lille, France.

[17] "Equations, Tables, and Charts for Compressible Flow," Rept. 1135, 1953, NACA.

[18] Ericsson, L. E. and Reding, J. P., "Stall Flutter Analysis," *Journal of Aircraft,* Vol. 10, No. 1, Jan. 1973, pp. 5-13.

[19] Ericsson, L. E. and Reding, J. P., "Aerodynamic Effects of Bulbous Bases," CR-1339, 1969, NASA.

[20] Reding, J. P. and Ericsson, L. E., "Loads on Bodies in Wakes," *Journal of Spacecraft and Rockets,* Vol. 4, No. 4, April 1967, pp. 511-518.

[21] Ham, N. D. and Garelick, M. S., "Dynamic Stall Considerations in Helicopter Rotors," *American Helicopter Society Jounral,* Vol. 13, April 1968, pp. 44-55.

[22] Ericsson, L. E. and Reding, J. P., "Dynamic Stall of Helicopter Blades," *American Helicopter Society Journal,* Vol. 17, No. 1, Jan. 1972, pp. 10-19.

[23] Crimi, P. and Reeves, B. L., "A Method for Analyzing Dynamic Stall of Helicopter Rotor Blades," AIAA Paper 72-37, San Diego, Calif.

[24] Ericsson, L. E. and Reding, J. P., "Analytic Prediction of Dynamic Stall Characteristics," AIAA Paper 72-682, Boston, Mass., 1972.

[25] Liiva, J., Davenport, F. J., Gray, L., and Walton, I. C., "Two-Dimensional Tests of Airfoils Oscillating Near Stall," USA AVLABS TR 68-13A, Vol. 1, April 1968.

[26] Ericsson, L. E. and Reding, J. P., "Dynamic Stall Analysis in Light of Recent Numerical and Experimental Results," AIAA Paper 75-26, San Diego, Calif., 1975.

[27] Harper, P. W. and Flanigan, R. E., "The Effect of Rate of Change of Angle of Attack on the Maximum Lift of a Small Model," TN 2061, 1949, NACA.

[28] Loving, D. L., "Wind-Tunnel-Flight Correlation of Shock-Induced Separation Flow," TND-3580, 1966, NASA.

[29] Stanewsky, E. and Hicks, G., "Scaling Effects on Shock-Boundary Layer Interaction in Transonic Flow," AFFDL-TR-68-11, March 1968, Air Force Flight Dynamics LAB., Wright-Patterson Air Force Base, Ohio.

[30] Hall, I. M. and Rogers, E. W. E., "The Flow Pattern on a Tapered Swept-Back Wing at Mach Numbers Between 0.6 and 1.6," Rept. 1969, 1957, Aeronautical Research Council, London.

[31] Rogers, E. W. E., Berry, C. J., and Townsend, J. E. C., "A Study of the Effect of Leading Edge Modifications on the Flow Over a 50-Deg Swept-back Wing at Transonic Speeds," R&M 3270, 1962, Aeronautical Research Council, London.

[32] Reding, J. P. and Ericsson, L. E., "Delta Wing Separation Can Dominate Shuttle Dynamics" *Journal of Spacecraft and Rockets,* Vol. 10, No. 7, July 1973, pp. 421-428.

[33] Erickson, L. L., "Transonic Single-Mode Flutter and Buffet of a Low Aspect Ratio Wing Having a Subsonic Airfoil Shape," TN D-7346, Jan. 1974, NASA.

[34] Lindsey, W. F. and Landrum, E. J., "Compilation of Information on the Transonic Attachment of Flows at the Leading Edges of Airfoils," TN 4204, Feb. 1958, NACA.

[35] Goetz, R. C., "Preliminary Results of a Reentry Shuttle Vehicle Wing Buffet and Stall Flutter Experimental Investigation," presented to the Space Shuttle Technology Coordinating Group: Dynamics and Aeroelasticity Technology Area, NASA Langley Research Center, Nov. 1969.

[36] Chevalier, H. L. and Robertson, J. E., "Pressure Fluctuations Resulting from Alternating Flow Separation and Attachment at Transonic Seeds," AEDC TDR 63-204, Nov. 1963, Arnold Engineering Development Center, Tullahoma, Tenn.

[37] Muhlstein, L. J., "Assessment of Potential Buffet Problems on the Space Shuttle Vehicle," *Proceedings of NASA Space Technology Conference,* 1972, TMX-2570, pp. 25-43, NASA.

[38] Ericsson, L. E. and Reding, J. P., "Dynamic Stall Simulation Problems," *Journal of Aircraft,* Vol. 8, No. 7, July 1971, pp. 579-583.

[39] Foster, D. N., "The Low-Speed Stalling of Wings with High-Lift Devices," AGARD-CPP-102, Paper 11, presented at the AGARD Specialists Meeting on Fluid Dynamics of Aircraft Stalling, Lisbon, Portugal, April 25-28, 1972.

[40] Moss, G. F., "Some Notes on the Aerodynamic Problems Associated with the Phenomenon of Buffeting," Tech. Memo. Aero 1293, Feb. 1971, Royal Aeronautical Establishment, London.

[41] Moss, G. F., Haines, A. B., and Jordan, R., "The Effect of Leading-Edge Geometry on High-Speed Stalling," AGARD-CPP-102, Paper 13, presented at the AGARD Specialists Meeting on Fluid Dynamics of Aircraft Stalling, Lisbon, Portugal, 1972.